

This article was downloaded by:

On: 25 January 2011

Access details: *Access Details: Free Access*

Publisher *Taylor & Francis*

Informa Ltd Registered in England and Wales Registered Number: 1072954 Registered office: Mortimer House, 37-41 Mortimer Street, London W1T 3JH, UK



Liquid Crystals

Publication details, including instructions for authors and subscription information:

<http://www.informaworld.com/smpp/title~content=t713926090>

A new series of siloxane liquid crystalline dimers exhibiting the antiferroelectric phase

Nils Olsson^a; Bertil Helgee^a; Gunnar Andersson^b; Lachezar Komitov^b

^a Department of Materials and Surface Chemistry, Chalmers University of Technology, Göteborg, Sweden

^b Department of Physics, Liquid Crystal Physics, Gothenburg University, SE-412 96, Gothenburg, Sweden

Gothenburg, Sweden

To cite this Article Olsson, Nils , Helgee, Bertil , Andersson, Gunnar and Komitov, Lachezar(2005) 'A new series of siloxane liquid crystalline dimers exhibiting the antiferroelectric phase', *Liquid Crystals*, 32: 9, 1139 – 1150

To link to this Article: DOI: 10.1080/02678290500268176

URL: <http://dx.doi.org/10.1080/02678290500268176>

PLEASE SCROLL DOWN FOR ARTICLE

Full terms and conditions of use: <http://www.informaworld.com/terms-and-conditions-of-access.pdf>

This article may be used for research, teaching and private study purposes. Any substantial or systematic reproduction, re-distribution, re-selling, loan or sub-licensing, systematic supply or distribution in any form to anyone is expressly forbidden.

The publisher does not give any warranty express or implied or make any representation that the contents will be complete or accurate or up to date. The accuracy of any instructions, formulae and drug doses should be independently verified with primary sources. The publisher shall not be liable for any loss, actions, claims, proceedings, demand or costs or damages whatsoever or howsoever caused arising directly or indirectly in connection with or arising out of the use of this material.

A new series of siloxane liquid crystalline dimers exhibiting the antiferroelectric phase

NILS OLSSON[†], BERTIL HELGEE[†], GUNNAR ANDERSSON[‡] and LACHEZAR KOMITOV^{*‡}

[†]Department of Materials and Surface Chemistry, Chalmers University of Technology, Kemivägen 4 SE-412 96, Göteborg, Sweden

[‡]Department of Physics, Liquid Crystal Physics, Gothenburg University, SE-412 96, Gothenburg, Sweden

(Received 12 January 2005; in final form 27 June 2005; accepted 27 June 2005)

In this paper, we report the study of a new series of symmetric chiral liquid crystalline siloxane dimers, their related monomers, and two of those monomers with heptamethyl-trisiloxane attached. All the dimers coupled with a trisiloxane show the SmC_A phase, which in several cases has a large tilt angle greater than 40° over a wide temperature range, as well as high spontaneous polarisation in the field-induced ferroelectric state. Spacer lengths of 3–6 and 11 carbons between the siloxane central unit and the mesogenic cores were used. Monomers with 3–6 carbons in the spacer showed only orthogonal phases while the monomer with an 11-carbon spacer, as well as the monomers with siloxane attached, have a high tilt angle ferroelectric phase. The materials were characterized by means of DSC, NMR, X-ray diffraction, electro-optical methods (tilt angle and texture characterization) and polarization measurements.

1. Introduction

Liquid crystals, the fourth state of matter, have been studied extensively since the beginning of the twentieth century. Most of these studies have dealt with monomeric (monomesogenic) systems, however, during the last two decades polymeric systems have also been extensively investigated. In addition to those major groups it is also possible to create many well defined oligomeric systems with very attractive properties resulting from the combination of polymeric and monomeric properties in the oligomeric materials [1–17]. The simplest of these are the dimeric systems. After Vorländer's report on the first dimeric liquid crystals [18], there was a long hiatus in the field, but activity has increased greatly in recent years. The mesogens in the dimers have been connected in several different ways although most studies thus far have been carried out on dimers where an alkylene chain has been used as the connecting group. These dimers are interesting both because they have markedly different physical properties from conventional low molar mass liquid crystals [4, 17] and because they are model compounds for main chain polymeric systems [4, 9, 17].

A promising method of forming dimers is to use a siloxane as the central connector. Theoretical and

empirical studies dealing with this class of liquid crystals have been reported [2, 5, 11–14, 19–24]. The dimers containing siloxane have shown exceptional promise, as they combine several features of interest for applications. For instance, Coles *et al.* have shown [2, 12–14, 19–21] that, when a siloxane core is introduced into a dimer, the siloxane bulkiness and phase segregation properties tend to give the system very high and relatively temperature-independent molecular tilt angles. In addition, the phase segregation that is induced increases the mechanical ruggedness of the system, as the layers of siloxane stabilize the smectic ordering and facilitate the achievement of bookshelf alignment [25]. However, each molecule is still fairly small, and the viscosity and switching times of the liquid crystal are very similar to those of a monomesogenic system with the same mesogens. As an interesting extra feature, Coles *et al.* [12, 14, 26] showed that when trisiloxane spacers were used between mesogens that normally form a ferroelectric phase, the resulting dimer tended to form an antiferroelectric phase.

Antiferroelectricity (AF) in liquid crystals, discovered by Chandani *et al.* [27, 28], has shown a great application potential and sparked considerable activity among scientists and engineers during the last decade. Compared with ferroelectric (F), antiferroelectric liquid crystals have been regarded as easier to handle in applications. However, a major problem in ferroelectric

*Corresponding author. Email: komitov@fy.chalmers.se

liquid crystal displays (FLCDs), as well as in antiferroelectric liquid crystal displays (AFLCDs), is the insufficient darkness of the field-off state. This comes from misalignment of the liquid crystal that causes a reduction of the displayed image contrast. While this problem is very difficult to solve for FLCDs, the use of systems with a molecular tilt of 45° in AFLCDs offer a possible solution [29]. It follows from the description of the optical properties of AFLCs given in [29, 30] that an AFLC sample aligned in the horizontal AF (HAF) state, with the smectic layer normal and molecules parallel to the confining solid substrates, will exhibit a zero birefringent state, i.e. the field-off state of the sample will be totally black when inserted between crossed polarizers, regardless of the position of the smectic layer normal with respect to the polarizer. However, materials with tilted smectic phases with a molecular tilt of 45° are very rare and, in addition, their molecular tilt is generally strongly temperature-dependent. An exception to this behaviour is seen in the siloxane dimers reported by Coles and co-workers [12–14] as well as in the monomer AFLC mixture synthesized by the group of R. Dabrowski [31]. These materials exhibit ferro- and antiferro-electric phases that possess high molecular tilt, close to 45° , which is temperature-independent over a broad temperature interval. Further studies and development of other siloxane dimers are thus very interesting both from a scientific point of view and with respect to specific applications.

The creation of AFLCs by incorporation of a siloxane central link between monomesogens, exhibiting ferroelectric properties, in the liquid crystal dimers, is an appealing way to greatly increase the variety of AFLC materials with high tilt angles, which is useful for further development of AFLCDs. Thus far, the flora of phases that these types of dimers show is far from being thoroughly investigated; in fact only a handful of mesogens have as yet been studied. In the systems studied the mesogens have been attached to a siloxane connector with long alkylene spacers, which ought to decrease the effect of the siloxane. It is therefore interesting to investigate dimers with very short spacers, and to identify whether this leads to any fundamental and unexpected changes in phase behaviour and physical properties. It has also been shown that using siloxane trimers as the connector between normally ferroelectric mesogens in the dimeric liquid crystals will not guarantee the formation of antiferroelectric phases; in some cases the system remains ferroelectric [22].

A versatile synthetic route to antiferroelectric, mechanically rugged liquid crystals with fast electro-optical response and high molecular tilt angles is needed

for AFLCD development. In this paper, the synthesis and liquid crystalline properties of 1,3-di(4-alkoxybiphenyl-4-carboxylic acid butyl ester)hexamethyltrisiloxanes with spacer lengths of 3–6 and 11 carbons, and the corresponding monomers are reported. For comparison we have included one tetrasiloxane dimer and two intermediate compounds with the trisiloxane, but as monomers instead of dimers, to try to differentiate between the siloxane effect and the effect from the dimeric structure as shown in scheme 1. The chiral centres of these liquid crystalline dimers are located near the periphery of the molecule to allow the chiral group great freedom of movement. Characterization using microscopic observation, powder X-ray, calorimetric and electro-optical methods were applied to deduce the phase behaviour and physical characteristics of the substances. All dimers with trisiloxane proved to be antiferroelectric. The long spacers gave a very broad SmC_A phase, which decreased as expected with shorter spacers, while the saturated apparent molecular tilt angle increased to 45° with the shortest spacers. It should be noted also that the siloxane-capped monomers showed 40° – 45° degrees apparent tilt angle, although, in the SmC^* phase.

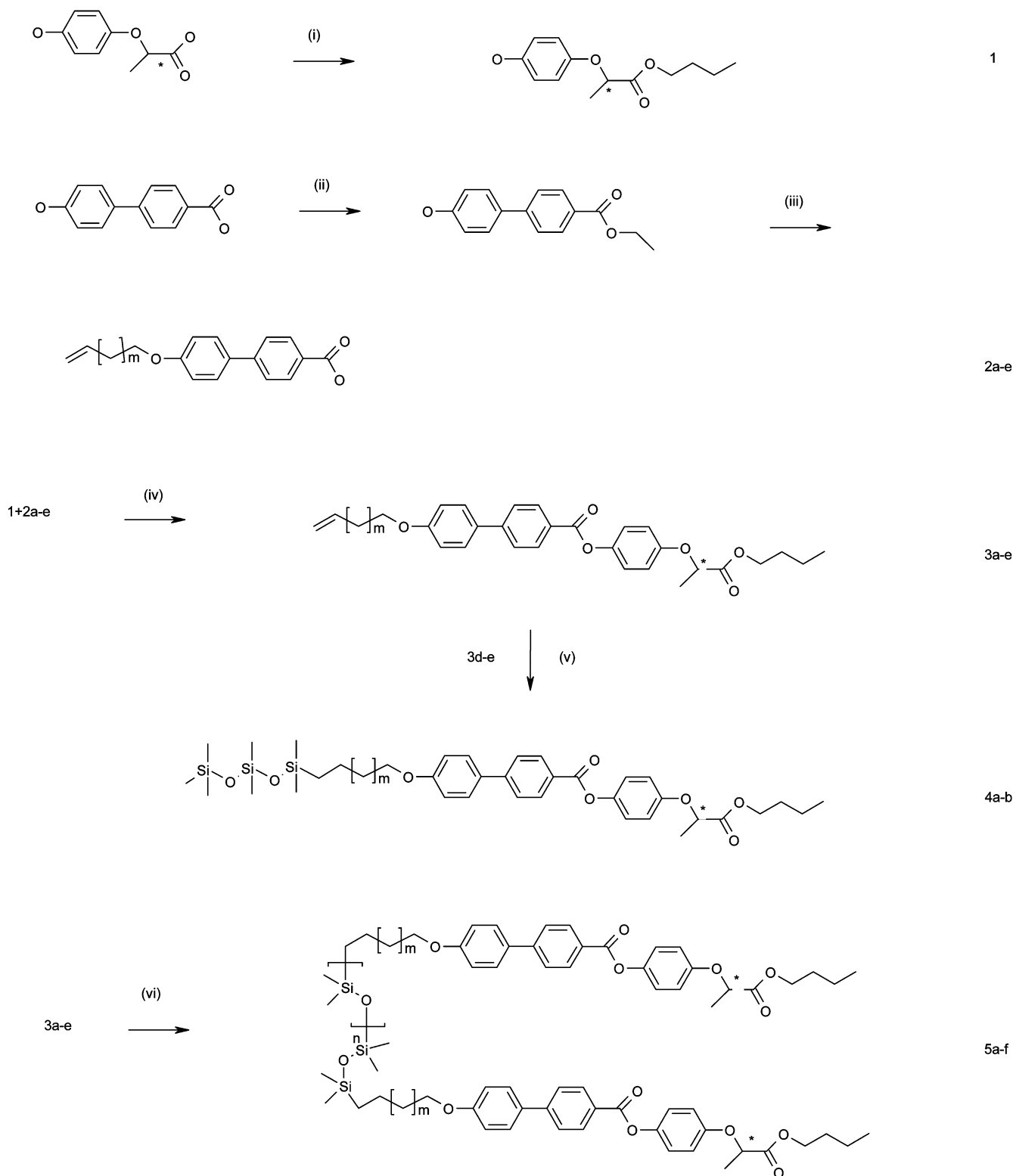
2. Experimental

The proposed structures of all the dimers and their intermediates were verified using 300 MHz ^1H NMR spectra obtained using a Varian VXR300 spectrometer. All spectra were run in CDCl_3 or $\text{DMSO}-d_6$ solutions. Infrared spectra were recorded on a Perkin-Elmer 1000 FTIR spectrophotometer using a BaF_2 cell for liquid phase IR and toluene as the solvent.

Materials and reagents were of commercial grade quality and used without further purification unless otherwise noted. Dry toluene and methylene chloride were obtained by passing the solvents through a bed of aluminium oxide (ICN Alumina N-Super I). (+)-2-(4-Hydroxyphenoxy)propionic acid was generously provided by BASF.

2.1. Synthesis

The synthesis of monomers **3a–e**, intermediate compounds **4a,b** and dimers **5a–f** was carried out according to the reactions shown in scheme 1. All structures were verified with ^1H NMR spectroscopy and NMR data were in accordance with the structures in all cases. The monomers and dimers described are all based on the central mesogenic unit derived from the phenoxypropanoic ester of biphenyl; after the synthetic part we will use the abbreviated name based on the PPB unit with numbers depending on the number of carbons in



Scheme 1. (i) BuOH, cyclohexane, PTSA; (ii) C₆H₆, EtOH; (iii) acetone, alkene bromide, K₂CO₃, followed by EtOH+NaOH; (iv) DCC/DMAP, CH₂Cl₂; (v) toluene, Pt-catalyst, 1-hydroheptamethyltrisiloxane; (vi) toluene, Pt-catalyst, dihydroxy siloxane.

the tail and spacer, and the number of silicon atoms in the siloxanes used.

2.1.1. 2-(*R*)-(4-Hydroxyphenoxy)propanoic acid butyl ester(1). A solution of 2-(*R*)-(4-hydroxyphenoxy)propanoic acid (0.11 mol, 20 g) in a mixture of butanol (300 ml) and cyclohexane (50 ml) was heated at reflux in a Dean–Stark apparatus with 2 g toluene-4-sulphonic acid monohydrate (PTSA) for 6 h. The reaction mixture was evaporated to dryness, and residue the dissolved in diethyl ether and washed with water. The ether phase was evaporated and the dry product purified by column chromatography on silica gel with petroleum ether/ethyl acetate 2/1 as eluant; yield 17.8 g (68%). ¹H NMR in CDCl₃, δ 0.88 (t, 3 H), 1.30 (m, 2 H), 1.6 (d+m, 5 H), 4.14 (m, 2 H), 4.65 (q, 1 H), 6.72 (m, 4 H).

2.1.2. 4'-Allyloxybiphenyl-4-carboxylic acid (2a). 4'-Hydroxybiphenyl-4-carboxylic acid (13.62 g, 0.063 mol) was dissolved in a mixture of 180 ml benzene, 500 ml ethanol and 4 g sulphuric acid. The solution was heated under reflux in a Dean–Stark apparatus for 20 h; the volume of the reaction mixture was reduced to 100 ml. It was then extracted with diethyl ether and the organic phase was washed with water. The ether phase was evaporated to dryness and the 4 g (16.5 mmol) of crude product was dissolved in 100 ml acetone with 2.42 g (20 mmol) allylbromide and 2.76 g (20 mmol) potassium carbonate. The mixture was heated under reflux with the exclusion of moisture for 4 days. It was then evaporated to dryness and the residue dissolved in diethyl ether. The solution was washed with water and evaporated to yield 94% of the ethyl ester of compound **2a**. ¹H NMR in CDCl₃ δ 1.43 (t, 3 H), 4.41 (q, 2 H), 4.61 (d, 2H), 5.33 (d, 1 H), 5.46 (d, 1 H), 6.1 (m, 1 H), 7.03 (d, 2H), 7.58(d, 2H), 7.63(d, 2H), 8.11 (d, 2H).

The 4'-allyloxybiphenyl-4-carboxylic acid ethyl ester (4.49) was dissolved in 300 ml ethanol, and 150 ml of NaOH (10%) in water was added. The solution was heated under reflux until all starting material had reacted, as monitored with TLC. It was then neutralized with HCl and the precipitate collected by filtration. It was washed with water and the aqueous phase extracted with diethyl ether. The dry precipitate and the product extracted to the ether phase were both collected for nearly quantitative yield. Other compounds **2** were made by analogous methods.

2.1.3. 4'-But-3-enyloxybiphenyl-4-carboxylic acid (2b). This synthesis used but-3-enylbromide; the purification

of the intermediate ester by column chromatography on silica gel was carried out with petroleum ether/ethyl acetate 3/1 as eluant; yield 52%. ¹H NMR in d8-DMSO δ 4.08 (t, 2H), 5.15 (m, 2 H), 5.9 (m, 1 H), 7.05 (d, 2H), 7.67 (2, 2H), 7.74 (d, 2H), 7.97 (d, 2H).

2.1.4. 4'-Pent-4-enyloxy-biphenyl-4-carboxylic acid (2c). This synthesis used pent-4-enylbromide; the crude product was directly refluxed in 200 ml ethanol and 100 ml 10% NaOH in water for 2 days. 25 ml HCl was added and the precipitated product collected on a filter and dried; yield 93%. ¹H NMR in d8-DMSO δ 1.8 (quintet, 2 H), 2.8 (q, 2 H), 4.0 (t, 2 H), 5.0 (m, 2 H), 5.8 (m, 1 H), 7.0 (d, 2 H), 7.66 (2, 2 H), 7.72 (d, 2 H), 7.98 (d, 2 H), 12.89 (s,1 H).

2.1.5. 4'-Hex-5-enyloxy-biphenyl-4-carboxylic acid (2d). Hex-5-enylbromide was used as starting material; the ester was purified by column chromatography on silica gel with toluene/ethyl acetate 20/1 as eluant. The product was refluxed in 200 ml ethanol/100 ml 10% NaOH/H₂O overnight; yield 78%. ¹H NMR in d8-DMSO δ 1.49 (m, 2 H), 1.75 (quintet, 2H), 2.09 (q, 2 H), 4.04 (t, 2 H), 5.0 (m, 2H), 5.82 (m, 1 H), 7.54 (d, 2 H), 7.67 (d, 2 H), 7.75 (d, 2 H), 7.98 (d, 2 H).

2.1.6. 4'-Undec-10-enyloxy-biphenyl-4-carboxylic acid (2e). Similar to the preparation of **2a** but using undec-10-enylbromide and purifying the produced acid by recrystallization from acetic acid and ethanol; yield 69%. ¹H NMR in d8-DMSO δ 1.2–1.5 (m, 12 H), 1.72 (quintet, 2H), 2.0 (q, 2 H), 4.21 (t, 2 H), 4.96 (m, 2H), 5.79 (m, 1 H), 7.03 (d, 2 H), 7.67 (d, 2 H), 7.75 (d, 2 H), 7.98(d, 2 H).

2.1.7. 4'-Allyloxybiphenyl-4-carboxylic acid 4-(1-butoxycarbonyl-1-(*R*)-ethoxy)phenyl ester, 4PPB3 (3a). Acid **2a** (0.85 g, 2.4 mmol), compound **1** (0.53 g, 2.4 mmol) and 10 mg of dimethyl aminopyridine (DMAP) in dry methylene chloride were treated with 4.8 mmol (1 g) dicyclohexylcarbodiimid (DCC) at 0°C. The mixture was allowed to warm to room temperature and stirring was continued for 3 h. Dry glassware was used. Column chromatography on silica gel with toluene/ethyl acetate 20/1 as eluant gave 0.95 g of pure product; yield 87%. ¹H NMR in CDCl₃ δ 0.93 (t, 3 H), 1.35(m, 2 H), 1.6 (d+m, 5 H), 4.19 (t, 2 H), 4.61 (d, 2H), 4.76 (q, 2H), 5.33 (d, 1 H), 5.46 (d, 1 H), 6.1 (m, 1 H), 6.94 (d, 2H), 7.04 (d, 2H), 7.15 (d, 2H), 7.61(d, 2H), 7.69(d, 2H), 8.23 (d, 2H).

Other compounds **3** were made by analogous methods from the corresponding compound **2**.

2.1.8. 4'-[11-(1,1,2,2,3,3,3-Heptamethyltrisiloxanyl)undecyloxy]biphenyl-4-carboxylic acid 4(1-butoxycarbonylethoxy)phenyl ester, (4PPB11)3Si (4b). Compound **3e** (128 mg, 0.225 mmol), 55 mg 1-hydroheptamethyltrisiloxane (0.25 mmol) and 0.6 μ mol platinum divinyltetramethyldisiloxane as catalyst were dissolved in 5 ml of dry toluene in a flask fitted with a CaCl₂ drying tube. The reaction mixture was stirred at room temperature overnight. The completion of the reaction was checked by monitoring the disappearance of the Si–H stretch at 2120 cm⁻¹. Column chromatography on silica gel with toluene/ethyl acetate gradient as eluant gave 163 mg of pure product; yield 91.5%. ¹H NMR in CDCl₃ δ 0.02–0.1 (m, 21 H), 0.53 (m, 2H), 0.91 (t, 3 H), 1.3–1.6 (m, 23 H), 1.82 (m, 2H), 4.01 (t, 2 H), 4.20 (t, 2H), 4.75 (q, 1H), 6.93 (d, 2H), 7.0 (d, 2H), 7.14 (d, 2H), 7.59(d, 2H), 7.68(d, 2H), 8.22 (d, 2H).

2.1.9. 1,1,2,2,3,3-Hexamethyl-1,5-bis(3'-propyloxybiphenyl-4-carboxylic acid 4(1-butoxycarbonyl-1-(*R*)-ethoxy)phenyl ester)trisiloxane, di(4PPB3)3Si (5a). Compound **3a** (89 mg, 0.195 mmol), 19.9 mg (0.095 mmol) 1,5-dihydrohexamethyltrisiloxane and 0.2 μ mol platinum divinyltetramethyldisiloxane as catalyst were dissolved in 3 ml of dry toluene in a flask fitted with a CaCl₂ drying tube. The reaction mixture was stirred at room temperature overnight. The completion of the reaction was checked by monitoring the disappearance of the Si–H stretch at 2120 cm⁻¹. Column chromatography on silica gel with toluene/ethyl acetate gradient as eluant gave 98 mg of pure product; yield 91%. ¹H NMR in CDCl₃ δ 0.08 (s, 6 H), 0.13 (s, 12 H), 0.73 (m, 4H), 0.93 (t, 6 H), 1.35(m, 4 H), 1.6 (d+m, 10 H), 1.92 (m, 4H), 4.06 (t, 4 H), 4.18 (t, 4H), 4.76 (q, 2H), 6.94 (d, 4H), 7.04 (d, 4H), 7.15 (d, 4H), 7.61(d, 4H), 7.69(d, 4H), 8.23 (d, 4H).

Other compounds **5** were made by similar methods.

2.1.10. 1,1,2,2,3,3,4,4-Octamethyl-1,7-bis(11'-undecyloxybiphenyl-4-carboxylic acid 4(1-butoxycarbonyl-1-(*R*)-ethoxy)phenyl ester)tetrasiloxane, di(4PPB11)4Si (5f). This was prepared from **3e** and 1,7-dihydro-octamethyltetrasiloxane similarly to **5a**; yield 62%. ¹H NMR in CDCl₃ δ 0.05 (s, 12 H), 0.08 (s, 12 H), 0.54 (m, 4H), 0.91 (t, 6 H), 1.3–1.6(m, 46 H), 1.82(m, 4H), 4.01 (t, 4 H), 4.20(t, 4H), 4.75(q, 2H), 6.93(d, 4H), 7.0(d, 4H), 7.14(d, 4H), 7.59(d, 4H), 7.68(d, 4H), 8.22 (d, 4H).

2.2. Characterization

The phase behaviour of the different materials under study was identified by a combination of optical microscopy, differential scanning calorimetry, electrical and electro-optical measurements. DSC measurements

were carried out with a Perkin-Elmer DSC 7 differential scanning calorimeter.

X-ray diffraction patterns were recorded using a Siemens D5000 diffractometer equipped with a Göbel mirror using Cu-K α radiation generated with a 45 kV, 45 mA current. The non-aligned samples were held in a thermostated Anton Paar TTK oven. Each data point was measured for 10 s, and angular steps of 0.05° in 2 θ were used between data points.

Optical microscopy studies were carried out on standard E.H.C. cells with gaps of 2, 4 and 6 μ m. The cells were filled with the liquid crystal material in the isotropic phase by capillary forces. The inner substrate surfaces of the cells, precoated with ITO transparent electrodes, were covered by a thin polyimide alignment layer rubbed unidirectionally. An alignment layer of this type usually imposes a planar alignment on most liquid crystals. The electro-optic studies were carried out in a set-up consisting of a polarizing microscope connected to a film camera and photo detector, oscilloscope, function generator with an amplifier and thermo-stage with temperature control within $\pm 0.1^\circ\text{C}$. The apparent tilt angle, θ_{app} , of the molecules, was determined from the electro-optical studies as half of the switching cone angle in the field-induced ferroelectric state with 1° uncertainty range. Spontaneous polarisation, P_s , of the field-induced ferroelectric state was measured using the Diamant bridge method [32].

3. Results and discussion

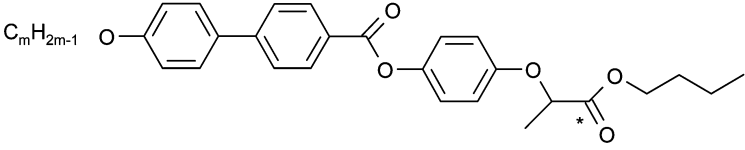
3.1. Monomers and their liquid crystal properties

As the monomers were not the focus of this study we made only a cursory characterization of their behaviour with the phase sequences shown in table 1.

3.1.1. 4PPB3 (3a). The monomer with the shortest spacer showed similar behaviour to 4PPB4 but was not carefully studied.

3.1.2. 4PPB4 (3b). The second shortest monomer had a SmA* focal-conic texture between 103 and 124°C and below that range the banded SmB* or E focal-conic texture appeared. As this phase stayed in the banded focal-conic texture all the way down to room temperature when cooled at 2°C min⁻¹, it is likely that it is the disordered crystal E phase. No crystallization was seen.

3.1.3. 4PPB5 (3c). On heating, this monomer shows a stable crystalline phase up to 104°C, where it forms an SmA* phase with a focal-conic texture up to 133°C.

Table 1. Transition temperatures of the monomers taken at heating/cooling; m denotes the number of carbon atoms in the spacer.


Compound	Treatment	m	Transition temperature/°C			
4PPB3	heating	3	Cr 105	SmA* 223	I	
4PPB4	heating	4	SmB*/E 103	SmA* 126	I	
4PPB5	heating	5	Cr 104	SmA* 133	I	
4PPB5	cooling	5	Cr 62	SmB*/E 91	SmA* 130	I
4PPB6	heating	6	Cr 79	SmA* 119	I	
4PPB6	cooling	6	Cr 61	SmB*/E 72	SmA* 116	I
4PPB11	heating	11	Cr 30	SmC* 74	SmA* 106	I

When cooled to 91°C a transition occurs to a phase very similar to the phase in 4PPB4, most likely E. In this material the E phase is monotropic and the material eventually crystallizes over the entire temperature region below the SmA* phase. To see crystallization in the E.H.C. cell the sample must be held in the range 80–90°C for a long time or cooled very slowly.

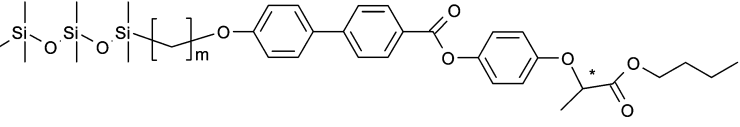
3.1.4. 4PPB6 (3d). The material with six carbons in the spacer shows the most complex phase diagram of the monomers when subjected to different heating and cooling rates. Cooling at 10°C min⁻¹ and heating again at 5°C min⁻¹ gives three different DSC peaks for different phases at 65.3, 73.8 and 79°C, but slow heating or cooling shows that only the last phase is thermodynamically stable. The two stable phases are a SmA* phase at 79–119°C and a crystal or more ordered SmX phase below 79°C in the DSC. However, as crystallization is hindered in the E.H.C cell we do not see crystallization in the microscope unless cooling proceeds very slowly. We see instead formation of a supercooled E/SmB* phase also in this case, with the typical banded focal-conic structure when cooled from the SmA* phase.

3.1.5. 4PPB11 (3e). The monomer with 11 carbons in the spacer has been studied previously [33]. It has a fairly wide SmC* phase at 30–74°C topped by an SmA* phase at 74–106°C. The spontaneous polarization is high; 300 nC cm⁻² was measured at 30°C.

The general feature of the monomers with six or fewer carbons in the alkylene spacer is that they form orthogonal phases, while the monomer with 11 carbons in the spacer forms a broad tilted phase below a SmA* phase. For this kind of series this is expected behaviour and may be rationalized in terms of rotational volume. The long alkane spacer will occupy a large rotational volume compared with that of the mesogenic core, which favours tilting of the mesogens. As expected, we also see a decrease of the clearing point temperature as the spacer length is increased. It is important to note that only 4PPB11 showed a tilted phase and that none of these materials is antiferroelectric.

3.2. Siloxane-capped monomers and their liquid crystal properties

Phase transition temperatures of these monomers are collected in table 2.

Table 2. Phase transition temperatures of the siloxane-capped monomers taken on heating; m denotes the number of carbon atoms in the spacer.


Compound	Treatment	m	Transition temperature/°C			
(4PPB6)3Si	heating	6	Cr 32	SmC* 66	I	
(4PPB11)3Si	heating	11	Cr -10	SmC* 92	SmA* 99	I

3.2.1. (4PPB6)3Si (4a). This siloxane-capped monomer shows a broad SmC* phase with a high tilt angle, saturating close to 45°, from 10 to 66°C as shown in figure 1, and a nearly linear increase in spontaneous polarization as shown in figure 2.

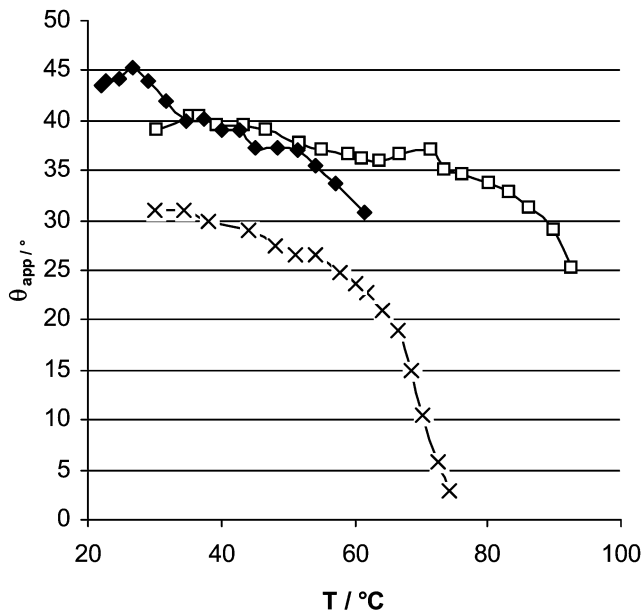


Figure 1. Apparent tilt angle θ_{app} of the siloxane-capped monomers as a function of temperature compared with the θ_{app} of 4PPB11: (4PPB6)3Si (\blacklozenge); (4PPB11)3Si (\square); 4PPB11 (\times).

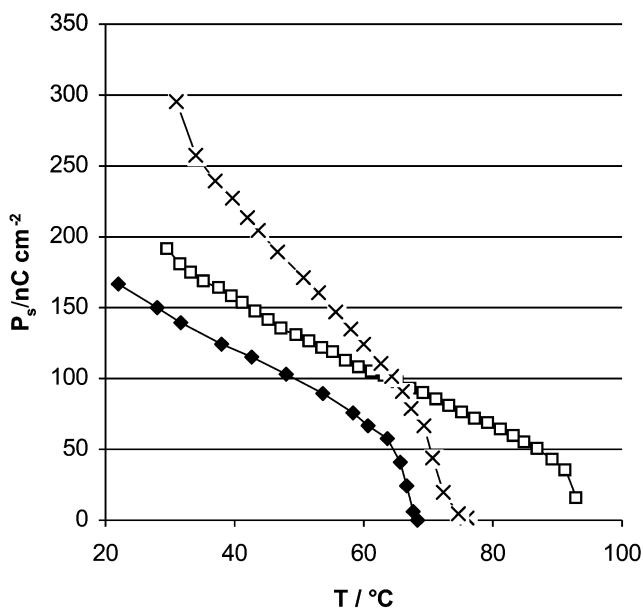


Figure 2. Spontaneous polarization of the monomers as a function of temperature: (4PPB6)3Si (\blacklozenge); (4PPB11)3Si (\square); 4PPB11 (\times).

3.2.2. (4PPB11)3Si (4b). The longest of all the monomers also shows a very broad SmC* phase and a SmA* phase in the range 92–99°C. This usually means that the tilt angle is smaller over the whole temperature region and starts at low angles at the SmA*/SmC* transition. As that is not the case in this material it seems possible that the SmA* phase is partly of the de Vries type with randomly tilted mesogens in the same way as 4PPB11, (4PPB11)2Si and di(4PPB11)3Si studied in [34].

As shown in figures 1 and 2, the two monomers that have been capped with heptamethyltrisiloxane show reduced temperature dependency of the spontaneous polarization as well as tilt angle compared with 4PPB11 itself. The tilt angles for the siloxane-capped monomers are higher than for 4PPB11. The polarization, however, is reduced somewhat by inclusion of the siloxane unit. It should be noted in this context that Sunohara *et al.* has published a paper on siloxanes similar to these with only three carbon spacers, and the resulting mesophase was only a few degrees wide [35].

3.3. Dimers and their liquid crystal properties

Phase transition data for these dimers are collected in table 3.

3.3.1. di(4PPB3)3Si, (5a). This material shows complex phase behaviour. The highly ordered crystalline phase melts at 79°C to give an isotropic liquid which on supercooling forms an antiferroelectric phase at 59°C; on cooling at 10°C min⁻¹ this phase continues down to 33°C, where a more ordered phase is formed. A lower cooling rate changed the phase transition temperatures only very slightly, except that the more ordered phase occurred earlier, at 45°C, at a 0.2°C min⁻¹ cooling rate. When the sample had been cooled from isotropic to the antiferroelectric phase, it was possible to induce a more ordered low temperature phase by applying an electric field. Otherwise, if the sample was not subjected to an electric field, the sample remained indefinitely in the antiferroelectric phase and hence did not behave like a typical supercooled phase. The texture of the antiferroelectric and field-induced ferroelectric domains is also clearly visible when the material has gone into the more ordered low temperature phase. This phase, however, does not react to an electric field. The apparent tilt angle, θ_{app} , measured in the field-induced ferroelectric state of the antiferroelectric phase is as close to 45° as could be measured.

3.3.2. di(4PPB4)3Si (5b). The dimer with four carbons in the spacer exhibited a highly ordered tilted phase on

Table 3. Phase transition temperatures of the dimers taken on heating/cooling; m denotes the number of carbon atoms in the spacer. di(4PPB11)4Si has a tetrasiloxane central unit while the others have a trisiloxane centre unit.

Compound	Treatment	m	Transition temperature/ $^{\circ}\text{C}$			
di(4PPB3)3Si	heating	3	Cr 79	I		
di(4PPB3)3Si	cooling	3	X 33	SmC _A 59	I	
di(4PPB4)3Si	cooling	4	X < 25	SmC _A 68	I	
di(4PPB5)3Si	heating	5	X 76	SmC _A 91	I	
di(4PPB6)3Si	heating	6	X 17	SmC _A 90	SmC* 96	I
di(4PPB11)3Si	heating	11	X 30	SmC _A 108	SmA* 122	I
di(4PPB11)4Si	heating	11	X 29	SmC* 113	SmA* 123	I

heating to the clearing point and a monotropic SmC_A phase from 68 $^{\circ}\text{C}$ down to room temperature when cooled at 5 $^{\circ}\text{C min}^{-1}$. In this phase a high apparent tilt angle θ_{app} in the range 40–45 $^{\circ}$ is observed in virtually the entire SmC_A phase temperature region as seen in figure 3. This dimer shows the lowest switching threshold (AF–F) in this series of dimers, typically

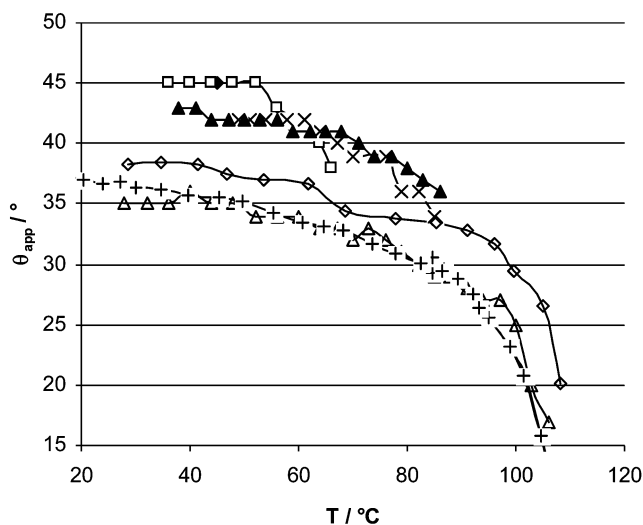


Figure 3. Apparent tilt angle θ_{app} of the dimers as a function of temperature. di(4PPB3)3Si (\blacklozenge); di(4PPB4)3Si (\square); di(4PPB5)3Si (\times); di(4PPB6)3Si (\blacktriangle); di(4PPB11)3Si (\triangle); 11-polymer (+); di(4PPB11)4Si (\diamond). Notice that the di(4PPB11)3Si (\triangle) and the 11-polymer (+) overlap almost completely in the same way as the di(4PPB5)3Si (\times) and di(4PPB6)3Si (\blacktriangle).

6 V μm^{-1} . When the higher ordered phase appears, the texture of this phase looks like a frozen variant of SmC_A if cooled without an applied electric field, and like an SmC* if cooled under a field, i.e. similar behaviour to that seen in di(4PPB3)3Si.

3.3.3. di(4PPB5)3Si (5c). As the spacer is extended to five carbons the stability of the less ordered phases increases as compared with the more ordered low temperature phase. The material shows an enantiotropic SmC_A phase in the range 76–91 $^{\circ}\text{C}$ in a DSC cell. The SmC_A phase is very easy to supercool and, even when cooled very slowly during the measurements in a 4 μm E.H.C. cell, the more ordered phase did not appear above 50 $^{\circ}\text{C}$. The apparent tilt angle, θ_{app} , is larger than 40 $^{\circ}$ for roughly half the temperature range of the SmC_A phase, and the SmC_A phase is very stable towards switching, with a typical threshold above 30 V μm^{-1} . At low temperatures, the field-induced SmC* phase relaxes very slowly back to the SmC_A phase and will eventually freeze in a tilted ordered phase. The SmC_A helix also appears to be comparatively stable, and about 18 V applied to a 4 μm cell is needed to unwind the helix.

3.3.4. di(4PPB6)3Si (5d). When the spacer length reaches six it is sufficiently long to give the material a very broad temperature range for the SmC_A phase and properties that are similar to those seen when the longest spacer is used in the di(4PPB11)3Si. It was

difficult to grow large uniformly aligned domains in a 4 μm cell of this material in the SmC_A phase. The sample texture consists of fairly small focal-conic domains. In spite of that, the sample exhibits a distinct preferred alignment direction. However, the uniform aligning of the LC became much easier in a 2 μm cell.

di(4PPB6)3Si has an enantiotropic SmC_A phase from room temperature to 88°C, topped by a SmC^* phase up to 96°C. As shown in figure 3, the tilt angles are large, larger than 40° from room temperature to 70°C.

There is a drastic change in the character of the current response of the sample at the temperature of the transition to SmC_A , from a clear single current peak of the current reversal in the SmC^* phase above 88°C to a typical example of an antiferro double current peak at lower temperatures. Just below 60°C, the antiferroelectric switching becomes less clear as it changes from finger-like solitary waves [36] to switching in very small domains that gradually become so small that it appears as a haze with a different birefringence that moves across the cell during a switch. There is a continuous decrease in the sharpness of the current peaks with decreasing temperature. This is due to an increasingly large tilt in the pretransitional region, which is also seen as a large change in the sample birefringence when a field is applied, before the switch to the field-induced ferroelectric state occurs.

3.3.5. di(4PPB11)3Si (5e). The precursor for this dimer has the longest spacer employed in this study and has previously been used to make side chain LC polysiloxanes [33]. It has several similarities to the side chain siloxane polymer with the same monomer unit. Both have approximately the same transition temperatures for the SmA^* as well as SmC^* phase, they have similar tilt angles and spontaneous polarization in the SmC^* phase (induced, in the dimer case). The important difference, however, is that di(4PPB11)3Si has the anticlinic SmC_A phase from room temperature to 108°C instead of the synclinic SmC^* phase of the polymer.

3.3.6. di(4PPB11)4Si (5f). This dimer has four siloxane units. It's behaviour is quite similar to the previously mentioned side chain LC polysiloxane [33]; which includes the presence of the ferroelectric SmC^* phase over a wide temperature range 29–113°C and SmA^* phase in the range 113–122.5°C.

3.4. Comparison of Liquid crystal properties

All the trisiloxane dimers in this study show antiferroelectric behaviour, low Δn of the field-off state and a

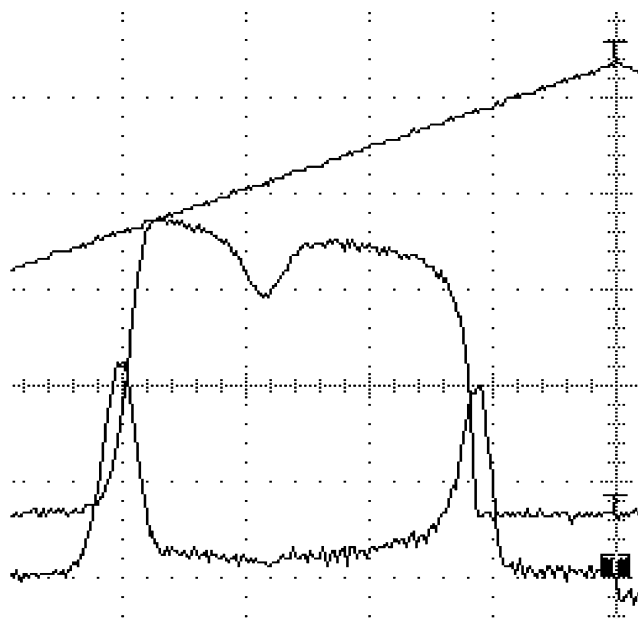


Figure 4. Typical electro-optical response of the dimers (snapshot taken at 55°C; the frequency of the applied triangle waveform field was 1 Hz.). The top line is a ramp of the applied electric field, the middle curve is the optical response, the bottom curve is the current response with the characteristic double peak. The dip in the optical response at low fields is due to the abrupt change of Δn caused by the Fréedericks transition at low voltages.

distinct double current peak, as seen in figure 4. For dimers with short spacers, 3, 4, 5 or 6 carbons (**5a–d**), the tilt angles θ_{app} are high, over 40°, while di(4PPB11)3Si (**5e**) shows a smaller tilt angle between 25° and 36°, as seen in figure 3 (and see table 4). This was somewhat surprising since a fairly similar dimer with a long spacer used in the studies by Coles *et al.* had close to a 45° tilt. However, in di(4PPB11)3Si there is a $\text{SmC}_A/\text{SmA}^*$ phase transition and it is common that tilted smectic phases formed from an SmA^* phase saturate at lower tilt angles compared with those that are formed from the isotropic phase. The two dimers with 11 carbons in the spacer, di(4PPB11)3Si and

Table 4. Condensed table of some important physical properties, 20°C below the transition to the SmC_A phase. T_C is the critical temperature of the transition to the SmC_A phase. $E_{\text{th}}^{\text{AF-F}}$ is the threshold for the field induced AF–F transition.

Compound	T_C - 20°C	P_s / nC cm^{-2}	Apparent tilt/°	$E_{\text{th}}^{\text{AF-F}}/\text{V } \mu\text{m}^{-1}$
di(4PPB4)3Si	48	278	45	6,24
di(4PPB5)3Si	71	230	39	35,5
di(4PPB6)3Si	76	148	39	7
di(4PPB11)3Si	88	80	29	8,75
di(4PPB11)4Si	93	70	33	

di(4PPB11)4Si, show great similarities to the side chain siloxane polymer made previously from the same side chain precursor [33]. The phase transition temperatures, spontaneous polarization and temperature dependence of the apparent tilt angle for the three systems using the 4PPB11 monomer are very similar. However, there is one important difference, di(4PPB11)3Si, the 4PPB11 dimer with a trisiloxane centre, exhibited the antiferroelectric state instead of the ferroelectric state.

One general and expected trend is that increasing spacer length increases the temperature range of the SmC_A phase. Short (3 or 4 carbons) spacers give only a monotropic SmC_A phase, 5 carbons in the spacer give a SmC_A phase in the range 71–86°C while 6 carbons in the spacer give a SmC_A phase between 17 and 90°C. That seems to be close to the maximum temperature range, as 11 carbons only increased the phase interval to 30–108°C. The added mobility with 11 carbons appears to cause a more ordered phase to appear at room temperature, which limits the working range of the SmC_A phase.

The smectic layer thicknesses, shown in figure 5, are consistent with each layer being formed by one tilted mesogen, being less than half the calculated length of the total dimer. Thus the dimers are either interdigitated, and in that case most probably V-shaped as Coles *et al.*, have suggested [12, 14, 19–21], or they are in a hairpin conformation. The hairpin conformation has been demonstrated by Zugenmaier in the X-ray study of a similar dimer in the crystal phase below the

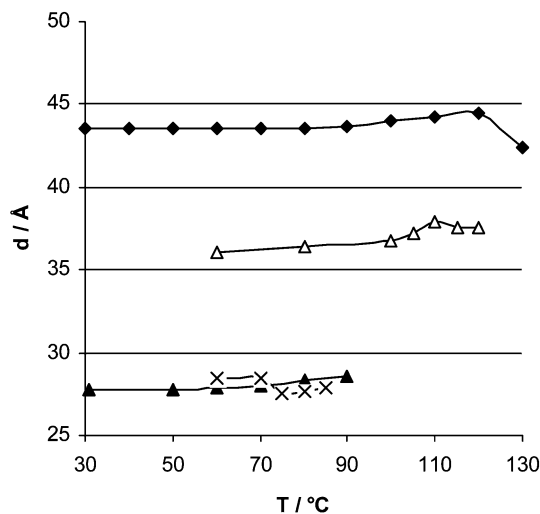


Figure 5. Smectic layer thickness d measured as a function of temperature for the trisiloxane dimers with 5 (\times), 6 (\blacktriangle) and 11 (\triangle) carbons in the spacer, as well as a comparison with the corresponding 4PPB11 on a side chain polysiloxane (\blacklozenge) containing twice as much siloxane as di(4PPB11)3Si. Below 70°C the d -value of the 5-dimer is influenced by crystallization.

antiferroelectric phase [23]. In the hairpin conformation the antiferroelectric order could be stabilized by steric effects, as steric lateral effects near the end of the mesogen have been shown to have a great influence on the antiferroelectric order [37]. It also seems possible that there is competition between the two types of ordering, and that both exist in the liquid crystalline phase; a simple sketch of such ordering is seen in figure 6. In a dielectric relaxation study [38] on another dimer, with an alkane chain constituting both linker and spacer, both forms had to be included in the model in order to explain their results. When comparing di(4PPB11)3Si with a side chain polysiloxane with the same mesogen and spacer, but with about twice the amount of siloxane as compared with the dimer, we see an increase in layer thickness of roughly 7 Å, while similar tilt angles are retained. This is approximately the length of three extra Si–O units and indicates that the system phase-segregates well, as all the extra siloxane volume seems to increase the layer thickness.

The apparent tilt angle is high for all the dimers and, as seen in figure 3, for the dimers with 3–6 carbons in the spacer it is greater than 40° over a broad temperature interval. A parallel study that we are presently conducting on a similar siloxane dimer that exhibits a broad antiferroelectric phase, indicates that the measured apparent tilt in the field-induced ferroelectric phase has the same magnitude as the molecular tilt in the antiferroelectric phase at field-off conditions. Hence, the dimers studied in this work, with exception of 4PPB11 dimers, are antiferroelectric liquid crystals whose molecular tilt is likely to exceed 40°. In contrast to most dimers made with high and relatively temperature independent apparent tilt angle, the spontaneous polarization of these materials is temperature dependent and decreases almost linearly with temperature, as shown in figure 7.

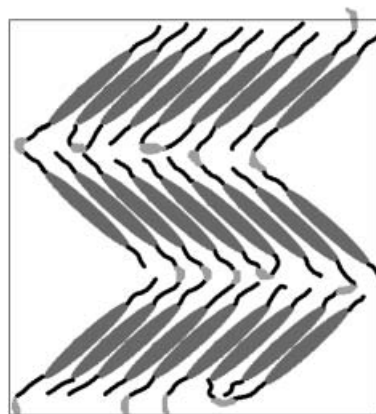


Figure 6. Sketch of a possible ordering of the dimers in the antiferroelectric phase.

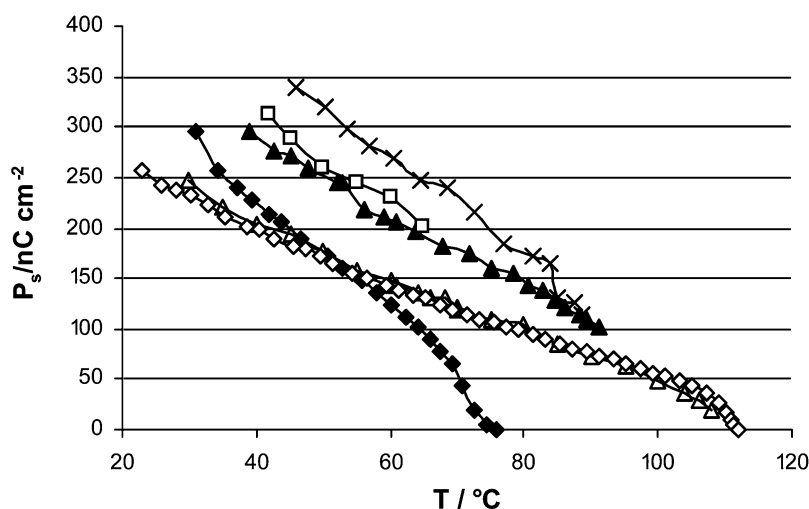


Figure 7. Spontaneous polarisation P_s measured as a function of temperature for the trisiloxane dimers with 5, 6 and 11 carbons in the spacer, compared with the 11-monomer without siloxane: di(4PPB4)3Si (\square); di(4PPB5)3Si (\times); di(4PPB6)3Si (\blacktriangle); di(4PPB11)3Si (\triangle); 4PPB11 (\blacklozenge); di(4PPB11)4Si (\diamond). Note the remarkably small difference between the two 11-dimers that almost completely overlap each other.

4. Conclusions

A new series of dimeric chiral antiferroelectric materials using a trisiloxane core has been synthesized together with their corresponding monomers. Spacer lengths of 3–6 and 11 carbons were used. To differentiate between the dimer effect and the siloxane effect in these systems, two monomers with 6 and 11 carbons in the spacer were capped with heptamethylsiloxane to produce two additional monomesogenic siloxane-containing compounds; also, a dimer with 11 carbons in the spacer and a tetrasiloxane core was synthesised. Monomers with 3–6 carbons in the spacer showed just orthogonal smectic phases, and only the long 11-carbon spacer monomer 4PPB11 gave a tilted smectic phase. The siloxane-capped monomers and di(4PPB11)4Si showed a SmC^* phase. All the other dimers, however, showed a SmC_A phase, as well as high spontaneous polarization in the field-induced ferroelectric state. Except for di(4PPB11)3Si, they also have very high apparent tilt angles, typically more than 40° over a large temperature range. In the phase diagram of di(4PPB11)3Si, there is a SmA^* phase above the tilted phase, which is consistent with the lower and more temperature-dependent tilt angle for that material. It is interesting to note that high tilt angles that are relatively temperature-independent compared with the monomer are also seen in the siloxane-capped monomers; this indicates that this effect is governed by the volume and segregation incompatibilities between the siloxane and the mesogenic parts, as discussed previously.

For the three systems based on 4PPB11, the tilt angle increases significantly with increasing siloxane content, with 4PPB11 having the lowest apparent tilt angle, di(4PPB11)4Si higher, and the highest apparent tilt shown by (4PPB11)3Si. The same trend is seen in the series of trisiloxane dimers, where shorter spacers, and thus a larger proportion of siloxane, give higher apparent tilt angles. As mentioned above, antiferroelectric liquid crystal materials with a molecular tilt close to 45° are very attractive for display applications because of the high quality black state they can generate.

This study shows that using short spacers (compared with those that have been previously used in similar dimers) can provide materials with interesting properties for applications where high tilt angles are needed, although excessively short spacers will give too narrow phase temperature ranges. In this study the dimers with the longest spacers also had the smallest tilt angles, which is an unwanted effect for the mentioned applications. However, further work on the design and synthesis of siloxane AFLC dimers, as well as a proper selection and mixing of these single compounds, is required in order to obtain AFLC materials possessing a large molecular tilt, preferably 45° , and broad temperature range. The electro-optical response of the dimers in this study is described in detail in [39].

Acknowledgements

This work was supported by the Swedish Research Council and the Swedish Foundation for Strategic Research (SSF).

References

- [1] C. Schott, S.P. Perkins, H.J. Coles. *Mol. Cryst. liq. Cryst.*, **366**, 2567 (2001).
- [2] P. Lehmann, W.K. Robinson, H.J. Coles. *Mol. Cryst. liq. Cryst. Sci. Technol. A*, **328**, 221 (1999).
- [3] B. Musgrave, P. Lehmann, H.J. Coles. *Liq. Cryst.*, **26**, 1235 (1999).
- [4] C.T. Imrie, G.R. Luckhurst. *Handbook of Liquid Crystals* Vol. 2B, pp. 801–833 (1998).
- [5] E. Wischerhoff, R. Zentel. *Liq. Cryst.*, **18**, 745 (1995).
- [6] W. Weissflog, C. Lischka, S. Diele, I. Wirth, G. Pelzl. *Liq. Cryst.*, **27**, 43 (2000).
- [7] J. Watanabe, T. Izumi, T. Niori, M. Zenyoji, Y. Takanishi, H. Takezoe. *Mol. Cryst. liq. Cryst. Sci. Technol. A*, **346**, 77 (2000).
- [8] G. Dantlgraber, S. Diele, C. Tschierske. *Chem. Commun.*, 2768 (2002).
- [9] A.C. Griffin, T.R. Britt. *J. Am. chem. Soc.*, **103**, 4957 (1981).
- [10] C.V. Yelamaggad, A. Srikrishnat, D.S.S. Rao, S.K. Prasad. *Liq. Cryst.*, **26**, 1547 (1999).
- [11] M. Ibnelhaj, A. Skoulios, D. Guillon, J. Newton, P. Hodge, H.J. Coles. *Liq. Cryst.*, **19**, 373 (1995).
- [12] W.K. Robinson, P.S. Kloess, C. Carboni, H.J. Coles. *Liq. Cryst.*, **23**, 309 (1997).
- [13] P. Kloess, J. McComb, H.J. Coles. *Ferroelectrics*, **180**, 233 (1996).
- [14] W.K. Robinson, C. Carboni, P. Kloess, S.P. Perkins, H.J. Coles. *Liq. Cryst.*, **25**, 301 (1998).
- [15] I. Nishiyama. *Adv. Mater.*, **6**, 966 (1994).
- [16] D. Pocięcha, D. Kardas, E. Gorecka, J. Szydłowska, J. Mieczkowski, D. Guillon. *J. mater. Chem.*, **13**, 34 (2003).
- [17] Y.-I. Suzuki, T. Isozaki, S. Hashimoto, T. Kusumoto, T. Hiyama, Y. Takanishi, H. Takezoe, A. Fukuda. *J. mater. Chem.*, **6**, 753 (1996).
- [18] D. Vorlander. *Z. phys. Chem.*, **126**, 449 (1927).
- [19] E. Corsellis, D. Guillon, P. Kloess, H. Coles. *Liq. Cryst.*, **23**, 235 (1997).
- [20] C. Carboni, W.K. Robinson, S.P. Perkins, H.J. Coles. *Ferroelectrics*, **212**, 161 (1998).
- [21] C. Carboni, H.J. Coles. *Mol. Cryst. liq. Cryst. Sci. Technol. A*, **328**, 349 (1999).
- [22] A. Kaeding, P. Zugenmaier. *Liq. Cryst.*, **25**, 449 (1998).
- [23] P. Zugenmaier. *Liq. Cryst.*, **29**, 613 (2002).
- [24] D. Guillon, M.A. Osipov, S. Mery, M. Siffert, J.F. Nicoud, C. Bourgoigne, P. Sebastiao. *J. mater. Chem.*, **11**, 2700 (2001).
- [25] H.J. Coles, H.F. Gleeson, G. Scherowksy, A. Schliwa. *Mol. Cryst. liq. Cryst. Lett.*, **7**, 117 (1990).
- [26] C. Carboni, W.K. Robinson, S.P. Perkins, H.J. Coles. *Ferroelectrics*, **212**, 161 (1998).
- [27] A.D.L. Chandani, E. Gorecka, Y. Ouchi, H. Takezoe, A. Fukuda. *Jpn. J. appl. Phys. 2, Lett.*, **28**, L1265 (1989).
- [28] A.D.L. Chandani, T. Hagiwara, Y. Suzuki, Y. Ouchi, H. Takezoe, A. Fukuda. *Jpn. J. appl. Phys. 2, Lett.*, **27**, L729 (1988).
- [29] A. de Meyere, J. Fournier, H. Pauwels. *Ferroelectrics*, **181**, 1 (1996).
- [30] R. Beccherelli, S.J. Elston. *Liq. Crystals*, **25**, 573 (1998).
- [31] K. D'Have, A. Dahlgren, P. Rudquist, J.P.F. Lagerwall, G. Andersson, M. Matuszczyk, S.T. Lagerwall, R. Dabrowski, W. Drzewinski. *Ferroelectrics*, **244**, 115 (2000).
- [32] H. Diamant, K. Drenck, R. Pepinsky. *Rev. sci. Instr.*, **28**, 30 (1957).
- [33] B. Helgee, T. Hjertberg, K. Skarp, G. Andersson, F. Gouda. *Liq. Cryst.*, **18**, 871 (1995).
- [34] M. Reihmann, A. Crudeli, C. Blanc, V. Lorman, Y.P. Panarin, J.K. Vij, N. Olsson, G. Galli. *Ferroelectrics*, **309**, 111 (2004).
- [35] K. Sunohara, K. Takatoh, M. Sakamoto. *Liq. Cryst.*, **13**, 283 (1993).
- [36] J.-F. Li, X.-Y. Wang, E. Kangas, P.L. Taylor, C. Rosenblatt, Y.-I. Suzuki, P.E. Cladis. *Phys. Rev. B*, **52**, R13075 (1995).
- [37] I. Nishiyama, J.W. Goodby. *J. mater. Chem.*, **3**, 149 (1993).
- [38] D.A. Dunmur, G.R. Luckhurst, M.R. de la Fuente, S. Diez, M.A. Perez Jubindo. *J. chem. Phys.*, **115**, 8681 (2001).
- [39] N. Olsson, G. Andersson, B. Helgee, L. Komitov. *Liq. Cryst.* (in press).